diversity

MDPI

*Article*

# Biology, Genetic Diversity, and Ecology of *Nitzschia acidoclinata* Lange-Bertalot (Bacillariophyta)

**Veronika B. Bagmet, Shamil R. Abdullin *, Arthur Yu. Nikulin, Vyacheslav Yu. Nikulin and Andrey A. Gontcharov**

Federal Scientific Center of the East Asia Terrestrial Biodiversity, Far Eastern Branch of the Russian Academy of Sciences, 159, 100-Letia Vladivostoka Prospect, Vladivostok 690022, Russia
* Correspondence: crplant@mail.ru

**Abstract:** The diatom *Nitzschia acidoclinata* is a widespread eurybiontic alga. There is little information on its life cycle properties and cardinal points. To fill this gap, we analyzed six *N. acidoclinata* clones from a range of habitats in Asiatic Russia regarding their genetic diversity, morphology, morphometry, geography, and ecology. A comparison of 15 *N. acidoclinata rbc*L sequences sampled across its relatively wide distribution area and contrasting habitats revealed no distinct genotypes in the species. We demonstrated that the valve morphology, their length, and the sexual activity of the investigated clones varied depending on the phase of their life cycle. In this species, abrupt size reduction was observed. It was revealed that *N. acidoclinata* reproduced by pedogamy, and its auxosporulation was season-dependent and observed in spring and autumn only. The mating activity in our clones was detected only when the cell size was reduced to 9–22 μm in length. The available data on sexual reproduction in the genus *Nitzschia* suggest that neither clades nor subclades comprise pedogamous or anisogamous taxa at the same time. However, isogamy could occur in the same clade with either pedogamy or anisogamy. These data provide a fundamental basis for the development of *N. acidoclinata* mass cultivation and long-term maintenance in culture technologies.

**Keywords:** cardinal points; diatom; geography; habitat; life cycle; *Nitzschia acidoclinata*; plastid-encoded *rbc*L gene region; ultrastructure

**Citation:** Bagmet, V.B.; Abdullin, S.R.; Nikulin, A.Y.; Nikulin, V.Y.; Gontcharov, A.A. Biology, Genetic Diversity, and Ecology of *Nitzschia acidoclinata* Lange-Bertalot (Bacillariophyta). *Diversity* **2022**, *14*, 1133. https://doi.org/10.3390/d14121133

Academic Editor: Michael Wink

Received: 14 November 2022
Accepted: 15 December 2022
Published: 17 December 2022



## 1. Introduction

Representatives of Bacillariophyta are promising for industrial cultivation because they synthesize fatty acids, polysaccharides, pigments, nanosized siliceous structures, phenolic compounds, etc. [1–6]. However, the long-term maintenance of diatom clones is problematic due to the features of their life cycle that result in a cell size reduction during vegetative reproduction (the MacDonald-Pfitzer rule; [7,8]). The clone will ultimately die without sexual reproduction because there will be no size restitution, but the clone also 'dies' (i.e., loses its genetic identity) because of genetic recombination when sexual reproduction occurs.

Thus, after a few months or years (depending on the growth rate of culture and size reduction per cell division), the cells will reach their minimum viable size and then die. Culture maintenance strategies need to be developed based on information on the key features of the species' life cycle [9]. Therefore, studies on the diatom life cycle, including sexual reproduction and restoring the cell size, are relevant and important.

Life cycles of various diatom species have been previously characterized [7,9–16], and several life cycle phases were recognized. These are the pre-reproductive phase with only vegetative cell division and cell-size reduction; the reproductive phase (sexual reproduction, zygote (auxospore) growth, and the transformation of auxospores to the initial cell); and the post-reproductive phase—vegetative growth after sexual reproduction

[7,10]. Geithler [17] distinguished the cardinal points of a species—the maximum and minimum cell sizes corresponding to the upper and lower limits of auxosporulation (sexual reproduction) and noticed their constancy for a species with slight fluctuations. These cardinal points probably correspond to threshold levels of the metabolic activity of the nucleus, which determine the size limit of the cells for the species during auxospore formation, the limits of the maturity range, and the limit of cell reduction [7,17]. Therefore, information on cardinal points could be important for the development of methods for diatom maintenance in culture.

There are several main types of sexual processes in diatoms: isogamy—a zygote is formed due to the fusion of gametes that are similar in size (size isogamy), shape (morphological isogamy), and/or behavior (physiological isogamy) and formed in different gametangia cells; anisogamy—a zygote is formed by the fusion of gametes that differ in size (size anisogamy), shape (morphological anisogamy), and/or behavior (physiological anisogamy) and are formed in different gametangia cells; oogamy—a zygote is formed by the fusion of large immobile female gametes (eggs) with small, usually mobile male gametes (sperm), and the eggs and sperm are formed in different cells; and automixis—a zygote is formed due to the fusion of gametes (pedogamy) or haploid nuclei (autogamy) formed in one gametangium cell [7,18]. Automixis is the only homothallic mode of sexual reproduction; therefore, diatom species reproducing by automixis are more promising for biotechnology because they could be maintained in culture for a long time due to self-reproduction.

*Nitzschia* is one of the largest (about 900 species) and taxonomically complex genera among diatoms [19]. Its representatives are distributed throughout the world in marine and freshwater habitats, in soil, on rocks, in caves, etc. [20–22]. It has been shown that some species have biotechnological potential (e.g., *N. palea* (Kütz.) W. Smith [23–26], *N. laevis* Frenguelli [27,28], *N. frustulum* (Kütz.) Grun. [29], and some others [30,31]), but their use remains limited in practice. That is largely due to the scarce information on the species' life cycles, including the type of sexual reproduction and cardinal points. The number of species attributed to the traditional genus *Nitzschia* grows annually [32–34], but these taxa are often described based on the features of the valves' morphological structure only [21,35–37]. However, the morphological parameters of the valves often overlap between species, which hampers correct taxonomic assignment. This problem is exacerbated by morphological parameter/feature alterations during the life cycle [15,22,38].

*N. acidoclinata* Lange-Bertalot is a widespread species (marine, freshwater, soil, etc.) that was described relatively recently [39]. It is a member of the Bacillariacean clade 8A-I along with *N. perminuta* Grun., *N. costei* Tudesque, Rimet & Ector, *N. soratensis* E.A. Morales & M.L. Vis, and *N. fonticola* (Grunow) Grunow, sharing a complex gridle [19]. There is little information on the type of sexual reproduction and morphological alterations during the life cycles for the clade members. To fulfill these gaps, we isolated six clones of *N. acidoclinata* from Asiatic Russia to examine morphological variation during the life cycle, the characteristics of auxosporulation, and the mating system using light and electron microscopy. We documented the full size and shape range in the species and demonstrated that it reproduces sexually by pedogamy with no gene exchange between individuals. We also accessed the genetic diversity in *N. acidoclinata* accessions originating across the species range using *rbc*L data.

## 2. Materials and Methods

### *2.1. Sampling and Culture*

Six strains of *N. acidoclinata* from various habitats across the eastern part of Russia were used in the study (Figure 1 and Table S1). A map of the sample sites was made with SimpleMappr (http://www.simplemappr.net; accessed on 7 December 2022).


**Figure 1.** Map of sample sites. See the legend for details.

All samples were collected by standard methods [40,41]. Clonal cultures were established by micropipetting single cells [41] and cultured in a Waris-H liquid nutrient medium with silicate added [42] at 20–22 °C with an irradiance of light intensity of 17.9–21.4 µmol photons·m$^{-2}$ s$^{-1}$ with a 16:8 h light–dark period. The strains were maintained in the culture collection of the Laboratory of Botany in the Federal Scientific Center of East Asian Terrestrial Biodiversity, Russian Federation.

### *2.2. Microscopy*

The morphologies and morphometrics of the cells were examined using an Olympus BX 53 light microscope (LM) equipped with Nomarski DIC optics and an Olympus DP27 digital camera, and scanning electron microscopy (SEM) (Merlin, Carl Zeiss, Germany). For morphological studies, frustules were cleaned by oxidation with hydrogen peroxide, rinsed several times with distilled water, and mounted in an Elyashev medium [22,43] with a refractive index of 1.67–1.68. For SEM, the material was dried onto brass stubs and coated with chrome. The obtained morphometric data were processed using the software package Statistica 10.0 and Microsoft Office Excel 2007. The shape index was calculated by the formula: average length / average width [44].

The examination of chloroplast fluorescence in living algal cells was performed with LSM 510 META and LSM 710 LIVE confocal laser scanning microscopes (Carl Zeiss, Jena, Germany) at the Instrumental Centre of Biotechnology and Gene Engineering of FSCEATB FEB RAS. To visualize the position of the nucleus, cells were stained with DAPI (Molecular Probes, Eugene, OR, USA). Files with the 3D-captured images were recorded and analyzed with LSM 510 Release v.4.2 and ZEN 2011 software.

### *2.3. Mating Experiments*

To cross our clones, we inoculated aliquots in pairs into 45 mm Petri dishes and cultured them in a liquid medium under the conditions described above. The mixed cultures were examined daily with an inverted microscope for three weeks. Mating experiments were performed throughout four seasons (spring, summer, autumn, and winter). To stimulate sexual crossing, sea salt at a concentration of 2 mg/L was added to the mineral medium [10,45]. The stages of sexual reproduction were described according to Poulíčková & Mann [46] and Poulíčková et al. [47].

*2.4. DNA Extraction, Amplification, and Sequence Analysis*

For the DNA analysis, the unialgal culture was harvested during the exponential growth phase and concentrated by centrifugation. The total genomic DNA was extracted according to Abdullin et al. [48]. PCR amplification of the plastid-encoded *rbc*L gene region was carried out using the primers DPrbcL1 (5′-AAGGAGGAADHHATGTCT-3′) and DPrbcL7 (5′-AAASHDCCTTGTGTWAGTYTC-3′; [49]) with an Encyclo Plus PCR kit (Evrogen, Moscow, Russia). The PCR products were purified with ExoSAP-IT PCR Product Cleanup Reagent (Affymetrix, Santa Clara, CA, USA) and sequenced in both directions using an ABI 3500 genetic analyzer (Applied Biosystems, Foster City, CA, USA) with a BigDye terminator v3.1 sequencing kit (Life Technologies Corporation, Austin, TX, USA) and the same primers used for PCR. Sequences were assembled with Staden Package v. 1.4 [50], deposited into GenBank under the accession numbers OM423713–OM423718, and compared with others available in GenBank using BLAST search (https://blast.ncbi.nlm.nih.gov/Blast.cgi; accessed on 20 January 2022). MEGA v.7.0.26 [51] was used to estimate interspecific pairwise distances (*p*-distances).

*2.5. Phylogenetic Analysis*

A dataset was assembled using sequences retrieved from the NCBI and the dataset from Mann et al. [19]. The sequences (the taxa and accession numbers are given in the tree) were aligned in the SeaView program [52]. The final alignment consisted of 54 diatom sequences with 1446 aligned base positions. The best evolutionary model GTR+I+G was determined using jModelTest 2.1.1 [53]. Phylogenetic trees were constructed using maximum likelihood (ML) in RAxML-NG (https://raxml-ng.vital-it.ch/#/; accessed on 20 January 2022; [54]) and Bayesian inference (BI) in MrBayes v.3.1.2 [55]. In BI, four runs of four Markov chains were executed for 1 million generations, sampling every 100 generations for a total of 10,000 samples. The convergence of the chains was assessed, and stationarity was determined according to the 'sump' plot with the first 2500 samples (25%) discarded as burn-in; posterior probabilities were calculated from trees sampled during the stationary phase. The robustness of the ML trees was estimated by bootstrap percentages (BP; [56]) and posterior probabilities (PP) in BI. BP < 50% and PP < 0.95 were not considered.

## 3. Results

*3.1. Phylogenetic Tree of Plastid-Encoded rbcL Gene*

The chloroplast *rbc*L gene partial sequences (1435–1464 bp) obtained for six analyzed strains revealed three close related genotypes differing from each other in one base substitution. The first genotype was found in the strains VCA-49 and VCA-50 from the Republic of Sakha, the second in VCA-48 from the same place, and the third in strains VCA-7, VCA-52, and VCA-51, collected from the Krasnoyarsk Territory, Jewish Autonomous Region, and Primorsky Krai, respectively. The results of the BLAST searches showed that our isolates were highly similar to *N. acidoclinata* accessions (>99.85%).

Phylogenetic analyses based on 54 *rbc*L gene partial sequences representing the clades/subclades 8A-I, 8A-II, 8B, and 8C-II of Bacillariaceae [19] placed our strains into the *N. acidoclinata* clade (100/1.00 for BP/PP). Due to a minor sequence divergence, the relationships between the *N. acidoclinata* accessions remained unresolved (Figure 2). In the unrooted ML phylogenetic tree, *N. acidoclinata* was as a sister to larger clade comprised by the well-supported lineages (1) *N. soratensis* and *N. costei* (100/1.00); (2) N. *perminuta* (95/1.00); and (3) the three accessions *N.* cf. *fonticola*, *N.* cf. *soratensis*, and *N.* cf. *hantzschiana* (100/1.00). These lineages together with basally placed *N. fonticola* formed the 8A-I clade [19].

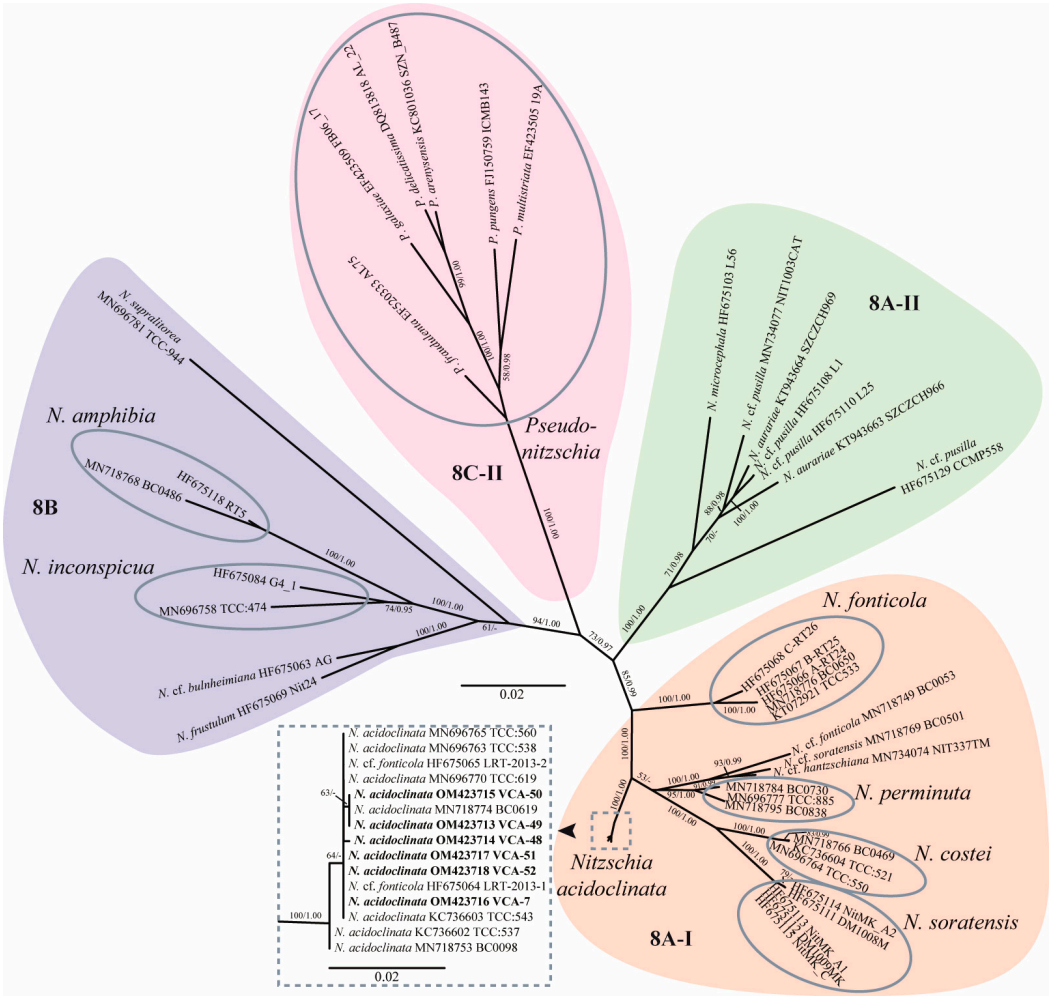


**Figure 2.** Unrooted ML tree showing the phylogenetic position of the new strains of *N. acidoclinata* based on plastid-encoded *rbc*L gene sequence data (GTR+I+G model). Support [ML/BI, (BP) ≥ 50% and (PP) ≥ 0.95] are given above/below the branches. Sequences obtained for this study are shown in boldface. Clade designations follow Mann et al. [19]. Scale bars—substitutions per nucleotide position.

### *3.2. Vegetative Cell Morphology*

The cells were solitary; no chains were formed (Figure 3A). All the frustules observed were Nitzschioid (i.e., with raphe systems diagonally opposed). The living cells contained two simple, elongated chloroplasts, one toward each pole (Figure 3A,B,D). During the interphase, the chloroplasts were appressed to the girdle, with their margins extending slightly onto the valves (Figure 3A,B,D). The interphase nucleus was centrally located (Figure 3C).

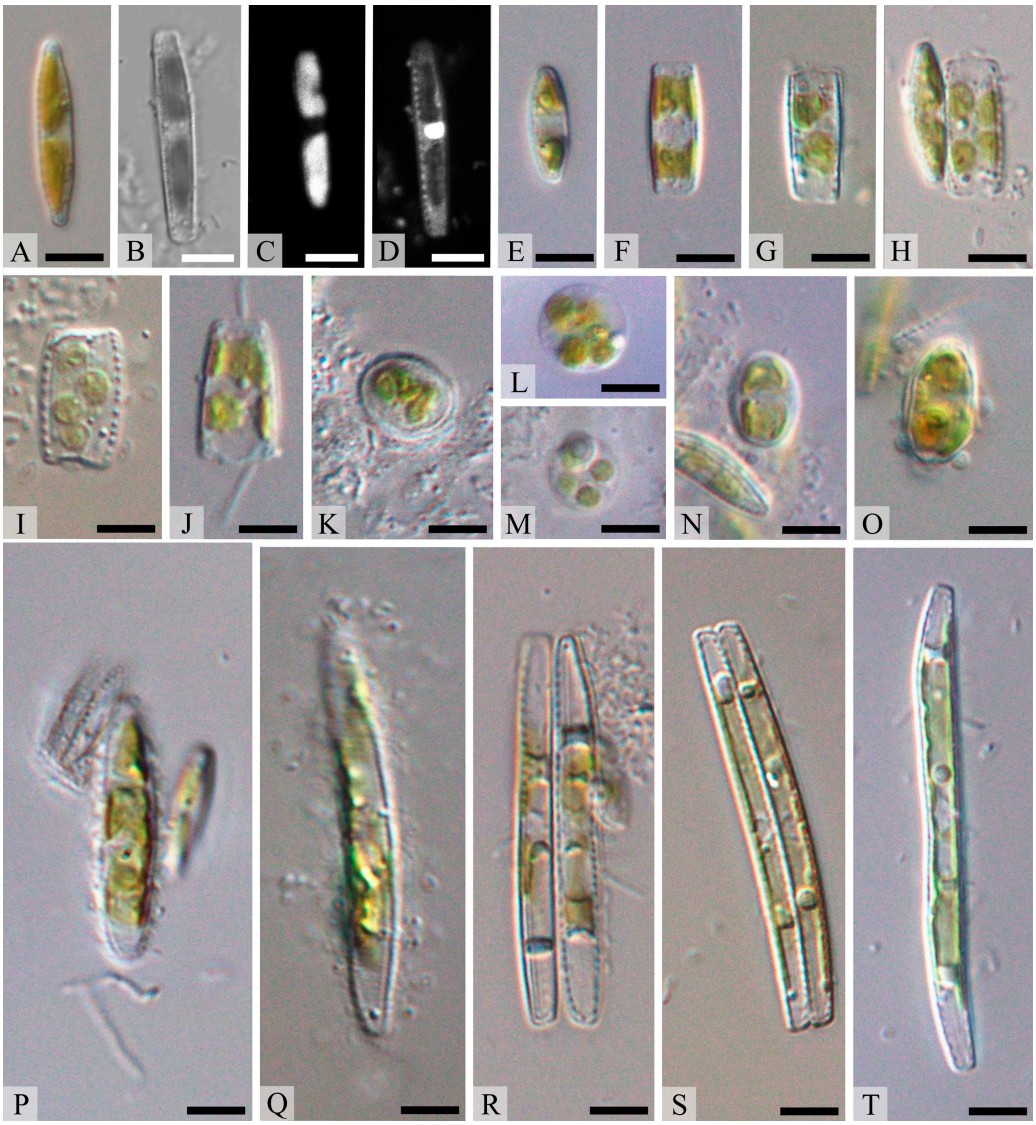


**Figure 3.** Life cycle of *N. acidoclinata*. (**A**–**D**) Vegetative cells, (**C**) nucleus, (**D**) chloroplasts, (**E**) cell before auxosporulation, (**F**) beginning of auxosporulation, (**G**,**H**) a cell with four chloroplasts, (**I**) contracted chloroplasts, (**J**,**K**) fusion of protoplasts (gametes) forming a zygote, (**K**) fusing of gametes forming a zygote, (**L**,**M**) abortion of a zygote, (**N**,**O**) auxospore germination from the zygote, (**P**,**Q**) releasing auxospore from the valves, (**R**–**T**) forming of initial cells; (**A**,**E**–**T**) light microscopy, (**B**–**D**) confocal laser scanning microscopy. Scale bars = 10 µm.

The morphological characteristics of *N. acidoclinata* are summarized in Table 1. The average lengths of the investigated strains were the most variable features, ranging from 10.5 (VCA-49, vegetative cells (VC)) to 47.1 µm (VCA-48, initial cells (IC)) (minimum—8.2 µm, VCA-7 (VC); maximum—52.3 µm, VCA-48 (IC)) due to the size reduction during the life cycle. The range of average valve widths was narrow, from 2.6 (VCA-48 (IC), VCA-49 (IC), and VCA-51 (VC)) to 3.1 µm (VCA-7 (VC)) (minimum—2.3, VCA-49 (IC); maximum—3.5, VCA-7 (VC)). The shape index varied from 3.75 (VCA-49 (VC)) to 18.12 (VCA-48 (IC)). The average fibula density varied from 8.9 (VCA-48 (IC)) to 10.9 (VCA-50 (VC)) (minimum—8, VCA-7 (VC), VCA-7 (IC), VCA-48 (IC), VCA-49 (VC), and VCA-51 (VC); maximum—14, VCA-48 (VC)) in 10 µm, with the average stria density from 27.0 (VCA-7 (IC) and VCA-52 (VC)) to 29.9 (VCA-51 (VC) and VCA-50 (VC)) (minimum—26, VCA-7 (IC), VCA-48 (IC), and VCA-52 (VC); maximum—32, VCA-49 (VC), VCA-51 (VC), and VCA-50 (VC)) in 10 µm, and the average areolae density was from 34.8 (VCA-48 (VC)) to

41.7 (VCA-49 (VC)) (minimum—31, VCA-7 (IC); maximum—44, VCA-7 (VC) and VCA-50 (VC)) in 10 μm.

**Table 1.** Morphometric characteristics of *N. acidoclinata* observed in our strains and described in the literature.

| Strain | Valve Length (μm) | Valve Width (μm) | Fibulae (in 10 μm) | Striae (in 10 μm) | Areolae (in 10 μm) | Shape Index |
|---|---|---|---|---|---|---|
| | | | min–max (X ± s) | | | |
| VCA-7 (vegetative cells) | 8.2–15.9 (12.0 ± 1.7) (n = 30) | 2.6–3.5 (3.1 ± 0.3) (n = 30) | 8–12 (10.1 ± 1.2) (n = 30) | 28–31 (29.5 ± 1.1) (n = 30) | 34–44 (38.7 ± 2.8) (n = 30) | 3.87 |
| VCA-7 (initial cells) | 34.9–47.2 (40.1 ± 3.8) (n = 30) | 2.7–3.3 (2.9 ± 0.2) (n = 30) | 8–11 (9.5 ± 1.1) (n = 30) | 26–28 (27.0 ± 0.9) (n = 30) | 31–41 (37.9 ± 2.1) (n = 30) | 13.83 |
| VCA-48 (vegetative cells) | 18.6–21.5 (20.0 ± 0.9) (n = 30) | 2.6–3.1 (2.9 ± 0.1) (n = 30) | 9–14 (10.5 ± 1.3) (n = 30) | 27–29 (27.9 ± 0.7) (n = 30) | 32–38 (34.8 ± 1.8) (n = 30) | 6.90 |
| VCA-48 (initial cells) | 41.–52.3 (47.1 ± 3.4) (n = 30) | 2.5–2.9 (2.6 ± 0.1) (n = 30) | 8–10 (8.9 ± 0.8) (n = 30) | 26–29 (27.1 ± 1.1) (n = 30) | 32–37 (35.2 ± 1.6) (n = 30) | 18.12 |
| VCA-49 (vegetative cells) | 8.9–12.4 (10.5 ± 1.1) (n = 32) | 2.7–3.0 (2.8 ± 0.1) (n = 32) | 8–10 (9.0 ± 0.8) (n = 32) | 28–32 (29.8 ± 1.2) (n = 32) | 40–43 (41.7 ± 1.1) (n = 32) | 3.75 |
| VCA-49 (initial cells) | 43.2–45.2 (44.1 ± 0.6) (n = 30) | 2.3–3.0 (2.6 ± 0.2) (n = 30) | 9.5–10.6 (10.0 ± 0.4) (n = 30) | 28–31 (29.3 ± 1.0) (n = 30) | 40–42 (41.0 ± 0.7) (n = 30) | 16.96 |
| VCA-51 (vegetative cells) | 9.4–13.3 (10.6 ± 1.2) (n = 30) | 2.4–2.8 (2.6 ± 0.1) (n = 30) | 8–12 (10.5 ± 1.0) (n = 30) | 29–32 (29.9 ± 0.9) (n = 30) | 38–43 (40.0 ± 1.6) (n = 30) | 4.08 |
| VCA-51 (initial cells) | 45.0–49.3 (46.8 ± 1.3) (n = 30) | 2.5–3.0 (2.8 ± 0.1) (n = 30) | 10.0–11.7 (10.7 ± 0.4) (n = 30) | 28–31 (29.7 ± 0.8) (n = 30) | 37–42 (39.3 ± 1.6) (n = 30) | 16.71 |
| VCA-50 (vegetative cells) | 19.0–26.3 (23.5 ± 2.2) (n = 30) | 2.5–3.3 (2.8 ± 0.2) (n = 30) | 10–12 (10.9 ± 0.8) (n = 30) | 28–32 (29.9 ± 1.1) (n = 30) | 37–44 (40.0 ± 2.4) (n = 30) | 8.39 |
| VCA-52 (vegetative cells) | 17.3–19.5 (18.5 ± 0.7) (n = 30) | 2.6–2.9 (2.7 ± 0.1) (n = 30) | 10–11 (10.5 ± 0.5) (n = 30) | 26–28 (27.0 ± 0.9) (n = 30) | 33–37 (35.2 ± 1.3) (n = 30) | 6.85 |
| Lange-Bertalot [39] | 8–40 | 2–3 | 11–14 | 27–32 | nd | nd |
| Hofmann et al. [57] | 8–45 | 2.5–3 | 10–16 | 27–34 | nd | nd |

Notes: X—mean, s—mean error, n—number of measurements, nd—no data.

No difference in the valve ultrastructure between the clones was revealed. The striae on the valve face and inner part of the valve were of the same type (Figure 4A,B). The striae extended onto the mantle of the valve and formed a series of open poroids on the valve face (Figure 4C,E). The poroids were grouped in threes within the raphe canal on the outer sides of the valve (Figure 4A–C). There were from one to three single poroids in the proximal raphe region (Figure 4A–C). The raphe was straight and filamentous, and the distal ends of raphe terminated in the helictoglossae. A central nodule was visible in the central pore (Figure 4). The segmented cingulum contained four open bands (Figure 4C). The first (most advalvar) band was the widest, and its pars exterior was perforated by a single row of oval poroids (occluded by hymens). Bands two and three were narrower and appeared plain. Band four was about the same width as two and three, and its pars exterior was perforated by a single row of oval poroids (occluded by hymens) as in band

one. The poroids in bands one and four were approximately one and a half times denser than the valve striae (Figure 4C).

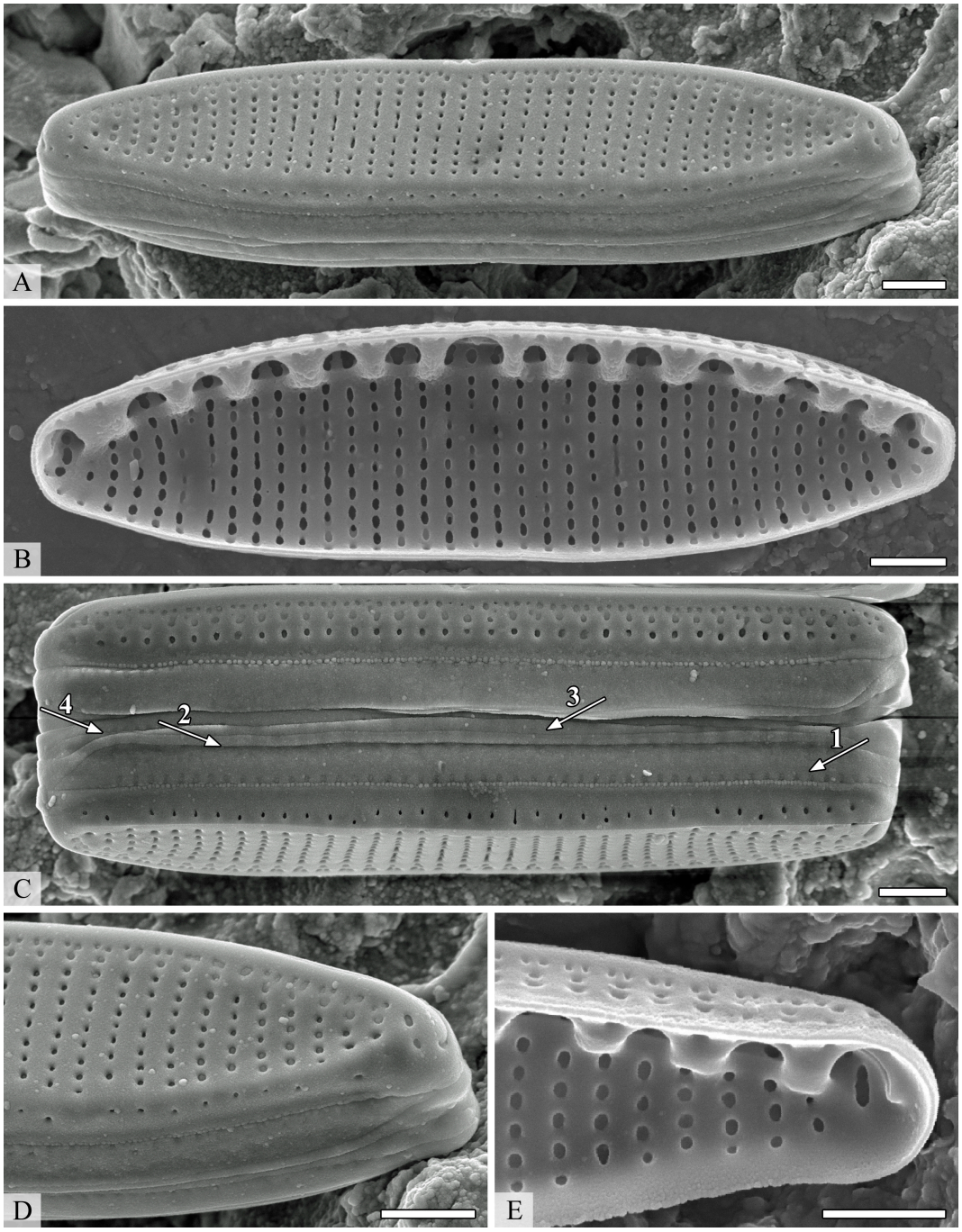


**Figure 4.** Cell ultrastructure of *N. acidoclinata*. (**A**) External valve view, (**B**) internal valve view, (**C**) girdle view of frustule showing the four open bands of the cingulum, (**D**) external view of the apex, (**E**) internal view of the apex. Scanning electron microscopy. Scale bars = 1 μm.

### *3.3. Auxosporulation*

Four strains (VCA-7, VCA-48, VCA-49, and VCA-51) showed sexual activity in the monoclonal cultures in the spring (February–March) and autumn (September–October). Sexual reproduction was marked in the third week from the start of the experiment. Sea salt addition to the culture medium did not stimulate initiation. No cell pairing was observed in the mixed cultures; instead, sexually active strains auxosporulated

independently. No mating was observed in strains VCA-50 and VCA-52 in monoclonal or mixed cultures.

Auxosporulation started from cell division that was not followed by the hypotheca formation and resulted in an increase in the girdle width (Figure 3F). Then, we observed frustules containing a cell with four chloroplasts, apparently produced by the fusion of the naked daughter protoplasts (Figure 3G,H). After that, the chloroplasts contracted (Figure 3I). Afterwards, the protoplasts (gametes) fused to form a zygote (auxospore) (Figure 3J,K). Initially, the valves remained associated with the zygote, but as the auxospore grew (Figure 3N,O), the valves opened and the auxospore was released (Figure 3P,Q) and formed the initial cell (Figure 3R–T), initiating the new generation. At times, zygote abortion without producing auxospores was observed (Figure 3L,M). Thus, *N. acidoclinata* reproduces sexually by pedogamy.

Young auxospores were ellipsoid (Figure 3N), gradually elongating along an axis that was nearly perpendicular to the parent cell, becoming first linear–ellipsoidal (Figure 3P), then linear (Figure 3Q). The initial cells often remained curved at the end of auxosporulation (Figure 3R–T). Such curvature and asymmetry of the cells disappeared during multiple vegetative divisions, which began immediately after the end of sexual reproduction.

## 4. Discussion

The morphology and ultrastructure of all *N. acidoclinata* clones agreed with the descriptions provided by Lange-Bertalot [39] and Hofmann et al. [57]. Our study revealed that this species was almost monomorphic in the metric characters studied in six clones. Moreover, a comparison of 15 *N. acidoclinata rbc*L sequences sampled across its relatively wide distribution area and contrasting habitats (e.g., marine and freshwater, soils, etc.) revealed no distinct genotypes in the species. We demonstrated that the valve morphology, their length, and sexual activity in all six investigated clones of *N. acidoclinata* varied depending on the phase of their life cycle (Figures 3 and 5, Table 1). The cells showed a progressive reduction of the length and valve shape from linear–lanceolate with retracted capitate apices and lanceolate with wedge-shaped apices to elliptical–lanceolate with rounded apices. The shape index showing these changes was higher in the initial cells than in vegetative cells (Table 1). Overall, the vegetative morphology of *N. acidoclinata* (e.g., the valve shape and ultrastructure, fibulae, striae and areolae densities, chloroplast number and position, etc.) did not allow for a confident discrimination of this species from *N. fonticola*. However, *N. acidoclinata* was distinct in the DNA sequence data that aided the correct taxonomic assignment.

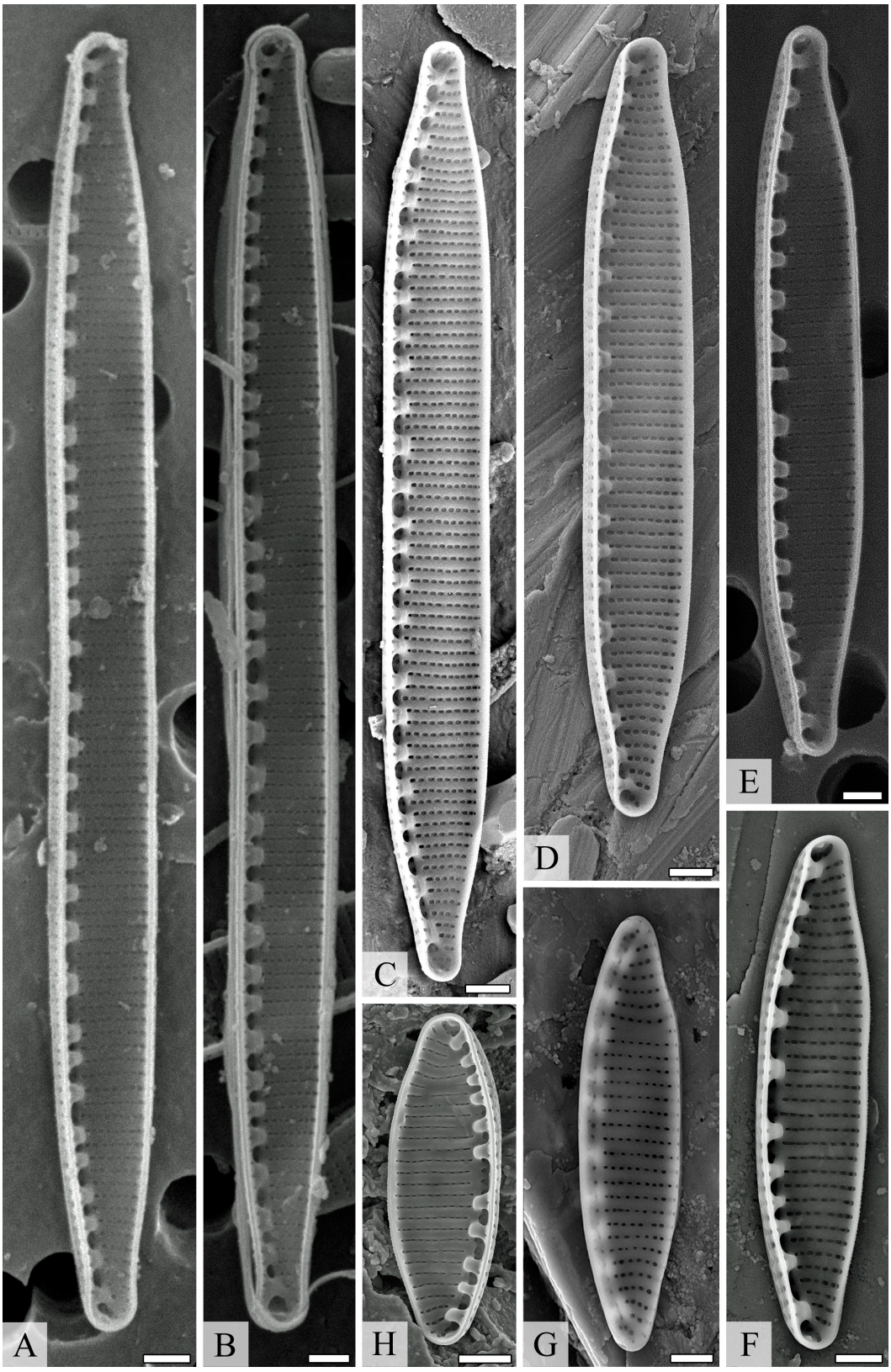


**Figure 5.** Valve morphology of the investigated *N. acidoclinata* clones. (**A**–**E**) linear–lanceolate valves with retracted capitate apices, (**F**,**G**) lanceolate valves with wedge-shaped apices, (**H**) elliptical–lanceolate valve with rounded apices. Scanning electron microscopy. Scale bars = 1 μm.

### *4.1. Reproductive Biology*

It was revealed that the life cycle involved sexual reproduction in most strains of *N. acidoclinata*. No pairing between cells was observed in crossing experiments. The clones produced auxospores via pedogamous automixis, an uncommon process among diatoms, which consists in self-fertilization within a single gametangium cell. *N. acidoclinata* auxosporulation was season-dependent and observed in spring and autumn only. Manipulations with salinity did not stimulate the start of the mating process, which causes the sexual process in some other diatom species [10,45].

Data on *N. acidoclinata* reproductive biology further extended the list of *Nitzschia* species characterized by automixis. Previously, pedogamy was characterized in *N. inconspicua* Grun. [58] and *N. fonticola* [15]. The latter species and *N. acidoclinata* are members of clade 8A-I, characterized by a complex gridle [19]. It is not clear whether automixis is a common feature for other species in this clade or not because there are no data on their reproductive biology features. *N. inconspicua* (clade 8B, characterized by a 'serial repeat' gridle) was only distantly related to *N. fonticola* and *N. acidoclinata* and it is unlikely that these species inherited automixis from the same common ancestor [9,15,58–60]. Yet, the characteristics of the mating systems and auxosporulation in *N. inconspicua* and *N. acidoclinata* were similar.

Among *Nitzschia* lineages, pedogamy was recorded only in subclades 8A-I and 8B. Isogamy was also observed in the subclade 8B, while anisogamy only in the subclade 6B. Both iso- and anisogamy are known in clade two [19]. Thus, the available data on sexual reproduction in the genus *Nitzschia* suggested that neither clades nor subclades comprise pedogamous or anisogamous taxa at the same time. However, isogamy could occur in the same clade with either pedogamy or anisogamy.

Oogamous sexual reproduction is typical for centric diatoms and most likely could be treated as a plesiomorphic feature that evolved to complete isogamy via anisogamy. Reproduction that involves two gametangial cells, each producing two gametes (anisogamy and isogamy), could be considered ancestral in pennates [61].

The phylogeny of the family Bacillariaceae [19] corroborates this hypothesis, implying that anisogamy was the ancestral type of sexual reproduction, while isogamy arose later, and, likely, pedogamy derived from isogamy. However, this evolutionary trend should be tested with more data on sexual reproduction in *Nitzschia*.

Auxosporulation involves little or no genetic recombination that may affect genetic diversity in the species. There have been no studies on diatoms specifically addressing this question, and any conclusions could be drawn only on the basis of mostly single-gene phylogenetic data collected so far. There were contrasting patterns of infraspecific diversity in *Nitzschia* pedogamous species. The minor *rbc*L sequence diversity observed in *N. acidoclinata* (15 accessions, *p*-distances 0.045% ± 0.025) corroborated assumptions about the reduced genetic diversity in organisms reproducing by self-fertilization. However, because *N. fonticola* and *N. inconspicua* have the same reproduction mode, the divergence was much higher (*p*-distance 0.59% ± 0.13, divergence 0.1–7.2%) [15,59].

### *4.2. Cell Size Reduction*

During vegetative division, sister cells complete their hypotheca, which leads to a gradual size reduction. However, in *N. acidoclinata*, abrupt size reduction was observed as well. During prolonged cultivation in individuals with asymmetrical and curved morphologies, the valves appeared due to the process of unequal vegetative division (Figure 6). The newly formed hypotheca made a sharp turn towards the valve of the sister cell and then, in the immediate vicinity of this valve, grew to the end of the cell. As a result, the cytoplasm was unequally distributed between the sister cells, which were 1.5–2.0 times smaller than the mother cell. This process has been described in diatoms (e.g., including *Tabularia tabulata* (C.Ag.) Snoeijs, *Licmophora ehrenbergii* (Kütz.) Grun., *Nitzschia lanceolata* W. Sm., *N. longissima* (Bréb.) Ralfs, and some others [7]) but is now reported for

*N. acidoclinata* for the first time. An abrupt size reduction could accelerate the transition of cells to a sexually mature state [7].

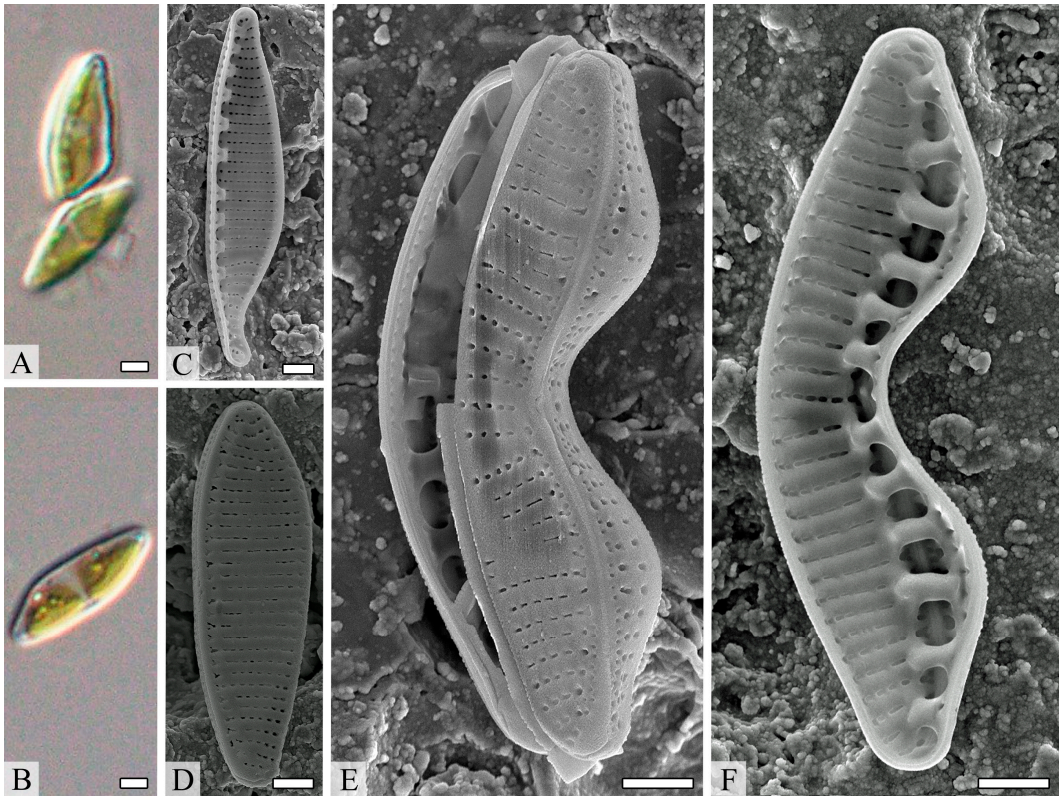


**Figure 6.** Cells of *Nitzschia acidoclinata* with asymmetrical and curved morphologies. (**A**,**B**) Light microscopy. Scale bars = 2 μm. (**C**–**F**) Scanning electron microscopy. Scale bars = 1 μm.

### *4.3. Cardinal Points*

The transition from vegetative cell division to sexual reproduction is size-dependent in diatoms [61]. No mating is possible if the cell length (pennate) or diameter (centric) is above specific critical limits called cardinal points [17,62]. According to Davidovich and Davidovich [61], the upper cardinal point is usually from 30 to 75% of the maximum species size. However, in about half of more than 70 species studied, the critical limit falls within a narrower range of 45 to 55%, and the general trend for a critical limit is 50%. *N. acidoclinata* somewhat deviated from this tendency, having an upper cardinal point in the range from 27% to 41%. The mating activity in our clones was detected only when the cell size was reduced to 9–22 μm in length during vegetative cell division.

The size range of the initial cells varied from 35 to 52 μm (Table 1). Interestingly, the size ranges provided by Lange-Bertalot [39] and Hoffman et al. [57] for this species (8–45 μm) fell within the ranges for lower and upper cardinal points, suggesting that populations studied by these authors were in the cell size range for sexualization, and some individuals recently underwent cell size restoration.

No sexual reproduction was observed in two clones (VCA-50 and VCA-52). In VCA-50, the length of some vegetative cells was above the upper cardinal point, which could be a reason for the lack of mating. However, the valve length in VCA-52 fit the cardinal point range identified for most clones of *N. acidoclinata* in this study.

### *4.4. Ecology and Geography*

*N. acidoclinata* was reported mostly from phytoplankton and bottom sediments in freshwater habitats [63–67]. Less frequently, the species was found in soils [68] and semi-terrestrial habitats, such as peatlands [69,70], with only one report from a marine habitat,

yet confirmed by the sequence data [71]. Four of our strains originated from waterlogged soils and two in the wet grounds of caves. Thus, this species could be regarded as eurybiontic.

The species apparently has a relatively wide distribution. It was found in Europe [64–66,68], Asia [67,69,70], and Africa [63], with no records from other continents. In Russia, *N. acidoclinata* was reported from the European part [72–74], Western Siberia [75–77], and the Far East [78,79]. Our data complemented the list of habitats and biogeographic data for this species.

## 5. Conclusions

The study of the biology, genetic diversity, and ecology of widespread *Nitzschia acidoclinata* (Bacillariophyta) allowed us to conduct precise taxa identification of natural clones; obtain the data on the valve morphology, their length, and the sexual activity of the species; observe the abrupt size reduction in *N. acidoclinata*; establish the mode of sexual reproduction as pedogamy (one of the forms of automixis; auxosporulation was season-dependent and observed in spring and autumn only); and add new data on the biogeography and ecology of the species. These data provide a fundamental basis for the development of *N. acidoclinata* mass cultivation and long-term maintenance in culture technologies.

**Supplementary Materials:** The following supporting information can be downloaded at: https://www.mdpi.com/article/10.3390/d14121133/s1, Table S1: origin data and GenBank accession numbers for the studied clones of *Nitzschia acidoclinata*.

**Author Contributions:** Conceptualization, supervision, project administration, and writing—review and editing, V.B.B. and S.R.A.; culture collection, strain setup and culturing, experiment, microscopic analysis, and data analyses, V.B.B.; writing—original draft preparation, A.A.G., S.R.A., A.Y.N., and V.Y.N.; molecular and phylogenetic analyses, A.Y.N. and V.Y.N.; visualization, V.B.B. and V.Y.N. All authors have read and agreed to the published version of the manuscript.

**Funding:** This study was supported by a grant from the Russian Science Foundation, RSF № 21-14-00196, https://rscf.ru/en/project/21-14-00196/; accessed on 12 November 2022.

**Institutional Review Board Statement:** Not applicable.

**Data Availability Statement:** The data presented in this study are available on request from the corresponding author. In addition, the data that support the findings of this study are openly available in GenBank.

**Acknowledgments:** The authors wish to express their gratitude to Sergey Zimov (Chersky Northeast Scientific Station, Pacific Geographical Institute, Far Eastern Branch, Russian Academy of Sciences) for the collecting of some samples, and Tatyana Gorpenchenko and Vitaliy Kazarin (Federal Scientific Center of East Asian Terrestrial Biodiversity, Far Eastern Branch, Russian Academy of Sciences) for their helping with confocal laser scanning and scanning electron microscopy.

**Conflicts of Interest:** The authors declare no conflicts of interest.

## References

1. Hemalatha, A.; Girija, K.; Parthiban, C.; Saranya, C.; Anantharaman, P. Antioxidant properties and total phenolic content of a marine diatom, *Navicula clavata* and green microalgae, *Chlorella marina* and *Dunaliella salina*. *Adv. Appl. Sci. Res.* **2013**, *4*, 151–157.
2. Davidovich, N.A.; Davidovich, O.; Podunai, Y.A.; Shorenko, K.I.; Kulikovskii, M.S. reproductive properties of diatoms significant for their cultivation and biotechnology. *Russ. J. Plant Physiol.* **2015**, *62*, 153–160. https://doi.org/10.1134/S1021443715020041.
3. Hess, S.K.; Lepetit, B.; Kroth, P.G.; Mecking, S. Production of chemicals from microalgae lipids–status and perspectives. *Eur. J. Lipid Sci. Technol.* **2018**, *120*, 1–26. https://doi.org/10.1002/ejlt.201700152.
4. Jin, C.; Yu, Zh.; Peng, Sh.; Feng, K.E.; Zhang, L.; Zhou, X. The characterization and comparison of exopolysaccharides from two benthic diatoms with different biofilm formation abilities. *An. Acad. Bras. Ciências* **2018**, *90*, 1503–1519. https://doi.org/10.1590/0001-3765201820170721.
5. Zhang, W.; Wang, F.; Gao, B.; Huang, L.; Zhang, C. An integrated biorefinery process: Stepwise extraction of fucoxanthin, eicosapentaenoic acid and chrysolaminarin from the same *Phaeodactylum tricornutum* biomass. *Algal Res.* **2018**, *32*, 193–200. https://doi.org/10.1016/j.algal.2018.04.002.

6. Akyil, S.; İlter, I.; Koç, M.; Demirel, Z.; Erdoğan, A.; Conk-Dalay, M.; Kaymak-Ertekin, F. Effects of Extraction Methods and Conditions on Bioactive Compounds Extracted from Phaeodactylum Tricornutum. *Acta Chim. Slov.* **2020**, *67*, 1250–1261. https://doi.org/10.17344/acsi.2020.6157.
7. Roshchin, A.M. Zhiznennye Tsikly Diatomovykh Vodoroslei (Life Cycles of Diatoms); Naukova Dumka Publishing House: Kiev, Ukraine, 1994; 171 p. (in Russian)
8. Edlund, M.B.; Stoermer, E.F. Ecological, evolutionary, and systematic significance of diatom life histories. *J. Phycol.* **1997**, *33*, 897–918.
9. Chepurnov, V.A.; Mann, D.G.; Sabbe, K.; Vyverman, W. Experimental studies on sexual reproduction in diatoms. *Int. Rev. Cytol.* **2004**, *237*, 91–154. https://doi.org/10.1016/S0074-7696(04)37003-8.
10. Drebes, G. Sexuality. In *The Biology of Diatoms: Botanical Monographs*; Werner, D., Eds.; Blackwell Scientific Publications: Oxford/England, UK, 1977; pp. 250–283.
11. Mann, D.G. Patterns of Sexual Reproduction in Diatoms. *Hydrobiologia* **1993**, *269*, 11–20. https://doi.org/10.1007/BF00027999.
12. Davidovich, N.A. Photoregulation of sexual reproduction in Bacillariophyta (review). *Int. J. Algae* **2002**, *4*, 56–71.
13. Amato, A.; Orsini, L.; D'Alelio, D.; Montresor, M. Life cycle, size reduction patterns, and ultrastructure of the pennate planktonic diatom *Pseudo-nitzschia delicatissima* (Bacillariophyceae). *J. Phycol.* **2005**, *41*, 542–556. https://doi.org/10.1111/j.1529-8817.2005.00080.x.
14. Trobajo, R.; Mann, D.G.; Cox, E.J. Sexual reproduction in *Nitzschia fonticola*: The importance of studying the entire life cycle in diatoms. *Phycologia* **2005**, *44*, 103.
15. Trobajo, R.; Mann, D.G.; Chepurnov, V.A.; Clavero, E.; Cox, E.J. Taxonomy, life cycle, and auxosporulation of *Nitzschia fonticola* (Bacillariophyta). *J. Phycol.* **2006**, *42*, 1353–1372. https://doi.org/10.1111/j.1529-8817.2006.00291.x.
16. Fuchs, N.; Scalco, E.; Kooistra, W.H.C.F.; Assmy, P.; Montresor, M. Genetic Characterization and life cycle of the diatom *Fragilariopsis kerguelensis*. *Eur. J. Phycol.* **2013**, *48*, 411–426. https://doi.org/10.1080/09670262.2013.849360.
17. Geitler, L. Der Formwechsel der pennaten Diatomeen (Kieselalgen). Archiv fur Protistenkunde **1932**, *78*, 1–226. (In German)
18. Davidovich, N.A. Definitions and concepts of reproductive biology of diatoms (terminological glossary). *Nov. Sist. Nizsh. Rast.* **2017**, *51*, 71–105. https://doi.org/10.31111/nsnr/2017.51.71.
19. Mann, D.G.; Trobajo, R.; Sato, S.; Li, C.; Witkowski, A.; Rimet, F.; Ashworth, M.P.; Hollands, R.M.; Theriot, E.C. Ripe for reassessment: A synthesis of available molecular data for the speciose diatom family Bacillariaceae. *Mol. Phylogenetics Evol.* **2021**, *158*, 106985. https://doi.org/10.1016/j.ympev.2020.106985.
20. Lin, C.S.; Chou, T.L.; Wu, J.T. Biodiversity of soil algae in the farmlands of mid-Taiwan. *Bot. Stud.* **2013**, *54*, 1–12. https://doi.org/10.1186/1999-3110-54-41.
21. Hamsher, S.E.; Kopalová, K.; Kociolek, J.P.; Zidarova, R.; Vijver, B.V. The genus *Nitzschia* on the South Shetland Islands and James Ross Island. *Fottea* **2016**, *16*, 79–102.
22. Bagmet, V.B.; Abdullin, S.R.; Mazina, S.E.; Nikulin, A.Y.; Gontcharov, A.A. Life cycle of *Nitzschia palea* (Kutzing) W. Smith (Bacillariophyta). *Russ. J. Dev. Biol.* **2020**, *51*, 106–114. https://doi.org/10.1134/S1062360420020022.
23. Binea, H.K.; Kassim, T.I.; Binea, A.K. Antibacterial activity of diatom *Nitzschia palea* (Kutz.) W. Sm. Extract. *Iraqi J. Biotechnol.* **2009**, *8*, 562–566.
24. Abdel-Hamid, M.I.; El-Refaay, D.A.; Abdel-Mogib, M.; Azab, Y.A. Studies on Biomass and Lipid Production of Seven Diatom Species with Special Emphasis on Lipid Composition of Nitzschia Palea (Bacillariophyceae) as Reliable Biodiesel Feedstock. *Algol. Stud.* **2013**, 143, 65–87. https://doi.org/10.1127/1864-1318/2013/0069.
25. Hassan, F.M.; Aljbory, I.F.; Kassim, T.I. An attempt to stimulate lipids for biodiesel production from locally isolated microalgae in Iraq. *Baghdad Sci. J.* **2013**, *10*, 97–108.
26. Abdullin, S.R.; Urazbakhtina, D.; Bagmet, V.B. Preliminary study of fungicidal and fungistatic activity of some cave microalgae. In Proceedings of the Abstracts of BIT's 3rd Annual International Congress of Algae-2014, Dalian, China, 16–18 October 2014; p. 203.
27. Wen, Z.Y.; Chen, F. A perfusion-cell bleeding culture strategy for enhancing the productivity of eicosapentaenoic acid by Nitzschia laevis. *Appl. Microbiol. Biotechnol.* **2001**, *57*, 316–322. https://doi.org/10.1007/s002530100786.
28. Wen, Z.Y.; Chen, F. Application of statistically-based experimental designs for the optimization of eicosapentaenoic acid production by the diatom *Nitzschia laevis*. *Biotechnol. Bioeng.* **2001**, *75*, 159–169. https://doi.org/10.1002/bit.1175.
29. Qin, T.; Gutu, T.; Jiao, J.; Chang, C.H.; Rorrer, G.L. Biological fabrication of photoluminescent nanocomb structures by metabolic incorporation of germanium into the biosilica of the diatom *Nitzschia frustulum*. *ACS Nano* **2008**, *2*, 1296–1304. https://doi.org/10.1021/nn800114q.
30. Kitano, M.; Matsukawa, R.; Karube, I. Changes in eicosapentaenoic acid content of Navicula saprophila, Rhodomonas salina and Nitzschia sp. under mixotrophic conditions. *J. Appl. Phycol.* **1997**, *9*, 559–563. https://doi.org/10.1023/A:1007908618017.
31. Jiang, A.; Ji, H.; Liu, H.; Zhu, H.; Ai, G.; Guo, X. Culture of benthic diatom *Nitzschia* sp. with macroalgae carriers and its application as feed of juveniles *Stichopus japonicus*. *Helgol. Mar. Res.* **2020**, *74*, 11. https://doi.org/10.1186/s10152-020-00544-7.

32. Witkowski, A.; Li, C.; Zgłobicka, I.; Yu, S.; Ashworth, M.; Dąbek, P.; Qin, S.; Tang, C.; Krzywda, M.; Ruppel, M.; et al. Multigene assessment of biodiversity of diatom(Bacillariophyceae) assemblages from the littoral zone of the Bohai and Yellow seas in Yantai region of Northeast China with some remarks on ubiquitous taxa. *J. Coast. Res.* **2016**, *74*, 166–195. https://doi.org/10.2112/SI74-016.1.
33. Suriyanti, S.N.P.; Usup, G. Morphology and molecular phylogeny of the marine diatom *Nitzschia dentatum* sp. nov. and *N. johorensis* sp. nov. (Bacillariophyceae) from Malaysia. *Bangladesh J. Plant Taxon.* **2017**, *24*, 183–196. https://doi.org/10.3329/bjpt.v24i2.35114.
34. Lobban, C.S.; Ashworth, M.P.; Calaor, J.J.M.; Theriot, E.C. Extreme diversity in fine-grained morphology reveals fourteen new species of conopeate *Nitzschia* (Bacillariophyta: Bacillariales). *Phytotaxa* **2019**, *401*, 199–238. https://doi.org/10.11646/phytotaxa.401.4.1.
35. Alakananda, B.; Mahesh, M.K.; Hamilton, P.B.; Supriya, G.; Karthick, B.; Ramachandra, T.V. Two New Species of *Nitzschia* (Bacillariophyta) from Shallow Wetlands of Peninsular India. *Phytotaxa* **2012**, *54*, 13–25. https://doi.org/10.11646/phytotaxa.54.1.2.
36. Álvarez-Blanco, I.; Blanco, S. Nitzschia imae sp. nov. (Bacillariophyta, Nitzschiaceae) from Iceland, with a redescription of *Hannaea arcus* var. *linearis*. *An. Jardín Botánico Madr.* **2013**, *70*, 144–151. https://doi.org/10.3989/AJBM.2358.
37. Liu, B.; Blanco, S.; Huang, B. Two new *Nitzschia* species (Bacillariophyceae) from China, possessing a canal-raphe-conopeum system. *Phytotaxa* **2015**, *231*, 260–270. https://doi.org/10.11646/phytotaxa.231.3.4.
38. Geissler, U. Die Schalenmerkmale der Diatomeen-Ursachen ihrer Variabilitat und Bedeutung fur die Taxonomie. *Nova Hedwig. Beih.* **1970**, *31*, 511–535. https://doi.org/10.1127/nova.beihefte/31/1970/511.
39. Lange-Bertalot, H. Eine revision zur taxonomie der *Nitzschiae lanceolatae* Grunow. Die "klassischen" bis 1930 beschribenen Süsswasserarten Europas. *Nova Hedwig.* **1976**, *28*, 253–307.
40. Kuzyakhmetov, G.G.; Dubovik, I.E. Metody Izucheniya Pochvennyh Vodorosley [Methods for Studying Soil Algae]; Izdatelstvo RIO BashGU: Ufa, Russia, 2001. (in Russian)
41. Andersen, R.A. *Algal Culturing Techniques*; Elsevier Academic Press: Burlington, MA, USA, 2005; ISBN 0-12-088426-7.
42. McFadden, G.I.; Melkonian, M. Use of Hepes buffer for microalgal culture media and fixation for electron microscopy. *Phycologia* **1986**, *25*, 551–557. https://doi.org/10.2216/i0031-8884-25-4-551.1.
43. Elyashev, A.A. *O prostom sposobe prigotovleniya vysokoprelomlyayushchej sredy dlya diatomovogo analiza* [On a simple method for preparing a highly refractive medium for diatom analysis]. *Tr. NII Geol. Arktiki* **1957**, *4*, 74–76. (In Russian)
44. Lange-Bertalot, H.; Ulrich, S. Contributions to the taxonomy of needle-shaped *Fragilaria* and *Ulnaria* species. *Lauterbornia* **2014**, *78*, 1–73.
45. Bagmet, V.B.; Abdullin, S.R.; Kuluev, B.R.; Davidovich, O.I.; Davidovich, N.A. The effect of salinity on the reproduction rate of *Nitzschia palea* (Kützing) W. Smith (Bacillariophyta) clones. *Russ. J. Ecol.* **2017**, *48*, 287–289. https://doi.org/10.1134/S1067413617030043.
46. Poulíčková, A.; Mann, D.G. Sexual reproduction in *Navicula cryptocephala* (Bacillariophyceae). *J. Phycol.* **2006**, *42*, 872–886. https://doi.org/10.1111/j.1529-8817.2006.00235.x.
47. Poulíčková, A.; Mayama, S.; Chepurnov, V.A.; Mann, D.G. Heterothallic auxosporulation, incunabula and perizonium in *Pinnularia* (Bacillariophyceae). *Eur. J. Phycol.* **2007**, *42*, 367–390. https://doi.org/10.1080/09670260701476087.
48. Abdullin, S.R.; Nikulin, A.Y.; Bagmet, V.B.; Nikulin, V.Y.; Gontcharov, A.A. New cyanobacterium *Aliterella vladivostokensis* sp. nov. (Aliterellaceae, Chroococcidiopsidales), isolated from temperate monsoon climate zone (Vladivostok, Russia). *Phytotaxa* **2021**, *527*, 221–233. https://doi.org/10.11646/phytotaxa.527.3.7.
49. Daugbjerg, N.; Andersen, R.A. Phylogenetic analyses of the rbcL sequences from haptophytes and heterokont algae suggest their chloroplasts are unrelated. *Mol. Biol. Evol.* **1997**, *14*, 1242–1251. https://doi.org/10.1093/oxfordjournals.molbev.a025733.
50. Bonfield, J.K.; Smith, K.F.; Staden, R. A new DNA sequence assembly program. *Nucleic Acids Res.* **1995**, *23*, 4992–4999. https://doi.org/10.1093/nar/23.24.4992.
51. Kumar, S.; Stecher, G.; Tamura, K. MEGA7: Molecular Evolutionary Genetics Analysis Version 7.0 for Bigger Datasets. *Mol. Biol. Evol.* **2016**, *33*, 1870–1874. https://doi.org/10.1093/molbev/msw054.
52. Galtier, N.; Gouy, M.; Gautier, C. SEAVIEW and PHYLO_WIN: Two graphic tools for sequence alignment and molecular phylogeny. *Bioinformatics* **1996**, *12*, 543–548. https://doi.org/10.1093/bioinformatics/12.6.543.
53. Darriba, D.; Taboada, G.L.; Doallo, R.; Posada, D. JModelTest 2: More models, new heuristics and parallel computing. *Nat. Methods* **2012**, *9*, 772. https://doi.org/10.1038/nmeth.2109.
54. Kozlov, A.M.; Darriba, D.; Flouri, T.; Morel, B.; Stamatakis, A. RAxML-NG: A fast, scalable and user-friendly tool for maximum likelihood phylogenetic inference. *Bioinformatics* **2019**, *35*, 4453–4455. https://doi.org/10.1093/bioinformatics/btz305.
55. Huelsenbeck, J.P.; Ronquist, F. MRBAYES: Bayesian inference of phylogenetic trees. *Bioinformatics* **2001**, *17*, 754–755. https://doi.org/10.1093/bioinformatics/17.8.754.
56. Stamatakis, A.; Hoover, P.; Rougemont, J. A rapid bootstrap algorithm for the RAxML web servers. *Syst. Biol.* **2008**, *57*, 758–771. https://doi.org/10.1080/10635150802429642.
57. Hofmann, G.; Werum, M.; Lange-Bertalot, H. *Diatomeen im Süßwasser-Benthos von Mitteleuropa*; Koeltz Scientific Books: Königstein, Germany, 2011. (In German)

58. Mann, D.G.; Sato, S.; Rovira, L.; Trobajo, R. Paedogamy and auxosporulation in *Nitzschia* sect. *lanceolatae* (Bacillariophyta). *Phycologia* **2013**, *52*, 204–220. https://doi.org/10.2216/12-077.1.
59. Rovira, L.; Trobajo, R.; Sato, S.; Ibáñez, C.; Mann, D.G. Genetic and physiological diversity in the diatom Nitzschia inconspicua. *J. Eukaryot. Microbiol.* **2015**, *62*, 815–832. https://doi.org/10.1111/jeu.12240.
60. Round, F.E.; Crawford, R.M.; Mann, D.G. *The diatoms: Biology and Morphology of the Genera*; Cambridge University Press: Cambridge, UK, 1990; 747 p, ISBN 978-0-521-36318-1.
61. Davidovich, N.A.; Davidovich, O.I. Reproduktivnaya biologiya diatomovykh vodorosley [Reproductive biology of diatoms]; LLC «Arial»: Simferopol, Russia, 2022. (in Russian)
62. Geitler, L. Die Auxosporenbildung von Nitzschia amphibian [The auxospore formation of Nitzschia amphibia]. *Osterr. Bot. Z.* **1969**, *117*, 404–410. (In German)
63. Archibald, R.E.M.; Schoeman, F.R. Taxonomic notes on diatoms (Bacillariophyceae) from the great usutu river in Swaziland. *South Afr. J. Bot.* **1987**, *53*, 75–92. https://doi.org/10.1016/S0254-6299(16)31478-8.
64. Ivanov, P.; Kirilova, E.; Ector, L. Diatom species composition from the river Iskar in the Sofia region, Bulgaria. In *Advances in Phycological Studies Festschrift in Honour of Prof. Dobrina Temniskova-Topalova*; Ognjanova-Rumenova, N., Manoylov, K., Eds.; Pensoft Publishers: Sofia, Bulgaria, 2006; pp. 167–190.
65. Kulikovskiy, M.S.; Genkal, S.I.; Mikheyeva, T.M. Novye dlya Belarusi vidy diatomovyh vodoroslej. 2. *Nitzschia* Hassall, *Hantzschia* Grunow i *Denticula* Kützing [New diatom species in belarus. 2. *Nitzschia* Hassall, *Hantzschia* Grunow and *Denticula* Kützing]. *Nat. Resour.* **2011**, *2*, 68–77 (in Russian)
66. Noga, T.; Stanek-Tarkowska, J.; Kochman, N.; Peszek, Ł.; Pajączek, A.; Woźniak, K. Application of diatoms to assess the quality of the waters of the Baryczka stream, left-side tributary of the river San. *J. Ecol. Eng.* **2013**, *14*, 8–23. https://doi.org/10.5604/2081139X.1055818.
67. Fang, J.; Liu, Y.; Wang, T.; Yan, X.; Shuo, Y.; Zhang, L.; Qu, Y. Estimation of organic pollution of the jinyaoshi lake based on the diatom assemblage of the lake sediments. *E3S Web Conf.* **2020**, *206*, 02007. https://doi.org/10.1051/e3sconf/202020602007.
68. Antonelli, M.; Wetzel, C.E.; Ector, L.; Teuling, A.J.; Pfister, L. On the potential for terrestrial diatom communities and diatom indices to identify anthropic disturbance in soils. *Ecol. Indic.* **2017**, *75*, 73–81. https://doi.org/10.1016/j.ecolind.2016.12.003.
69. Kulikovskiy, M.S.; Lange-Bertalot, H.; Witkowski, A.; Dorofeyuk, N.I.; Genkal, S.I. Diatom assemblages from Sphagnum bogs of the world. I. Nur bog in northern Mongolia. *Bibl. Diatomol.* **2010**, *55*, 1–326.
70. Chen, X.; McGowan, S.; Bu, Z.-J.; Yang, X.-D.; Cao, Y.-M.; Bai, X.; Zeng, L.-H.; Liang, J.; Qiao, Q.-L. Diatom-Based Water-Table Reconstruction in Sphagnum Peatlands of Northeastern China. *Water Res.* **2020**, *174*, 115648. https://doi.org/10.1016/j.watres.2020.115648.
71. Khaw, Y.S.; Khong, N.M.H.; Shaharuddin, N.A.; Yusoff, F.M.D. A simple 18S rDNA approach for the identification of cultured eukaryotic microalgae with an emphasis on primers. *J. Microbiol. Methods* **2020**, *172*, 105890. https://doi.org/10.1016/j.mimet.2020.105890.
72. Loseva, E.I.; Stenina, A.S.; Marchenko-Vagapova, T.I. Kadastr Iskopayemykh i Sovremennykh Diatomovykh Vodorosley Evropeyskogo Severo-Vostoka [Cadastre of the Fossil and Recent Diatoms from Northeastern Europe]; Geoprint: Syktyvkar, Russia, 2004. (in Russian)
73. Korneva, L.G. Fitoplankton Vodokhranilishch Basseyna Volgi [Phytoplankton of Volga River Basin Reservoirs]; Kostromskoy Pechatniy dom: Kostroma, Russia, 2015. (in Russian)
74. Chudaev, D.A.; Gololobova, M.A. Diatomoviye Vodorosli Ozera glubokogo (Moskovskaya Oblast') [Diatoms of Lake Glubokoe (Moscow Region)]; Tovarishchestvo Nauchnykh Izdaniy KMK: Moscow, Russia, 2016. (in Russian)
75. Lange-Bertalot, H.; Genkal, S.I. Diatoms from Siberia I. *Iconogr. Diatomol.* **1999**, *6*, 7–271.
76. Genkal, S.I.; Vekhov, N.V. Diatomovyye Vodorosli Vodoyemov Russkoy Arktiki: Arkhipelag Novaya Zemlya i Ostrov Vaygach [Diatoms of Water Bodies of the Russian Arctic: Novaya Zemlya Archipelago and Vaygach Island]; Nauka: Moscow, Russia, 2007. (in Russian)
77. Genkal, S.I.; Yarushina, M.I. Diatomoviye Vodorosli Slaboizuchennykh Vodnykh Ekosistem Kraynego Severa Zapadnoy Sibiri [Diatom Algae of Poorly Studied Aquatic Ecosystem in the Far North of Western Siberia]; Nauchniy Mir: Moscow, Russia, 2018. (in Russian)
78. Kharitonov, V.G. Diatomovyye Vodorosli Kolymy [Diatoms of the Kolyma]; Kordis: Magadan, Russia, 2014. (in Russian)
79. Genkal, S.I.; Gabyshev, V.A. Broadening the taxonomic composition of diatoms (Bacillariophyta) in the flora of the Lena river (streams of the Western slope of the Kharaulakh range, Yakutia). *Inland Water Biol.* **2021**, *14*, 349–356. https://doi.org/10.1134/S1995082921040064.